Received: 3 October 2022 | Revised: 7 November 2022 | Accepted: 29 November 2022

DOI: 10.1002/psp4.12901

ARTICLE

Predicting changes in the pharmacokinetics of CYP3A-metabolized drugs in hepatic impairment and insights into factors driving these changes

Mayur K. Ladumor[1] | **Flavia Storelli**[1] | **Xiaomin Liang**[2] | **Yurong Lai**[2] | **Osatohanmwen J. Enogieru**[3] | **Paresh P. Chothe**[4] | **Raymond Evers**[5] | **Jashvant D. Unadkat**[1]

[1]Department of Pharmaceutics, University of Washington School of Pharmacy, Seattle, Washington, USA

[2]Drug Metabolism, Gilead Sciences Inc., Foster City, California, USA

[3]Pharmacokinetics & Drug Metabolism, Amgen, South San Francisco, California, USA

[4]Global Drug Metabolism and Pharmacokinetics, Takeda Development Center USA, Inc., Lexington, Massachusetts, USA

[5]Preclinical Sciences and Translational Safety, Janssen Research & Development, LLC, Spring House, Pennsylvania, USA

Correspondence
Jashvant D. Unadkat, Department of Pharmaceutics, University of Washington School of Pharmacy, Seattle, WA 98195, USA.
Email: jash@uw.edu

Funding information
Amgen; Gilead; Janssen Pharmaceuticals; Takeda Pharmaceuticals U.S.A.

Abstract

Physiologically based pharmacokinetic models, populated with drug-metabolizing enzyme and transporter (DMET) abundance, can be used to predict the impact of hepatic impairment (HI) on the pharmacokinetics (PK) of drugs. To increase confidence in the predictive power of such models, they must be validated by comparing the predicted and observed PK of drugs in HI obtained by phenotyping (or probe drug) studies. Therefore, we first predicted the effect of all stages of HI (mild to severe) on the PK of drugs primarily metabolized by cytochrome P450 (CYP) 3A enzymes using the default HI module of Simcyp Version 21, populated with hepatic and intestinal CYP3A abundance data. Then, we validated the predictions using CYP3A probe drug phenotyping studies conducted in HI. Seven CYP3A substrates, metabolized primarily via CYP3A (fraction metabolized, 0.7–0.95), with low to high hepatic availability, were studied. For all stages of HI, the predicted PK parameters of drugs were within twofold of the observed data. This successful validation increases confidence in using the DMET abundance data in HI to predict the changes in the PK of drugs cleared by DMET for which phenotyping studies in HI are not available or cannot be conducted. In addition, using CYP3A drugs as an example, through simulations, we identified the salient PK factors that drive the major changes in exposure (area under the plasma concentration–time profile curve) to drugs in HI. This theoretical framework can be applied to any drug and DMET to quickly determine the likely magnitude of change in drug PK due to HI.

Study Highlights

WHAT IS THE CURRENT KNOWLEDGE ON THE TOPIC?

The ability of physiologically based pharmacokinetic (PBPK) models, populated with hepatic and intestinal drug-metabolizing enzyme and transporter

abundance, to accurately predict drug disposition in hepatic impairment (HI) has not been tested.

WHAT QUESTION DID THIS STUDY ADDRESS?

We validated the Simcyp Version 21 default HI PBPK model by comparing the model-predicted and the observed pharmacokinetic (PK) data for seven cytochrome P450 (CYP) 3A probe drugs. Then, through simulations, we elucidated the PK factors that drive the change in area under the plasma concentration–time curve (AUC) of CYP3A substrate drugs in HI.

WHAT DOES THIS STUDY ADD TO OUR KNOWLEDGE?

The PBPK model can predict, within twofold of the observed data, the PK of seven CYP3A substrate drugs in people with HI. Our theoretical simulations identified PK factors, that is, hepatic availability, gut availability, and fraction unbound in blood, that drive the large change in drug AUC in people with HI.

HOW MIGHT THIS CHANGE DRUG DISCOVERY, DEVELOPMENT, AND/OR THERAPEUTICS?

Such PBPK models could be used in the future to predict drug-dosing regimens or design PK studies in people with HI. The identified PK factors could be used to quickly determine the likely magnitude of change in drug AUC caused by HI.

INTRODUCTION

Liver cirrhosis or other liver diseases (collectively referred to as hepatic impairment [HI]) are the 11th and 15th leading causes of global death and morbidity, respectively.[1] The severity of HI is often classified using the Child–Pugh (CP) scores A (mild) to C (severe) based on clinical and laboratory variables (e.g., encephalopathy, ascites, serum bilirubin, serum albumin, prothrombin time).[2–4] HI causes changes in physiological parameters, such as drug-metabolizing enzyme and transporter (DMET) abundance in the liver, intestine, and other tissues; functional hepatic volume; hepatic blood flow ($Q_{B,H}$); biliary/renal clearance (CL); hematocrit; and drug-binding plasma proteins (e.g., albumin).[5–8] In addition, regardless of the CP score, changes in these physiological parameters can be disease dependent. For example, the change in the expression of DMET in the liver depends on the etiology of the disease (e.g., alcoholic vs. hepatitis C cirrhosis).[7,9–13]

Alteration of hepatic function and other physiological parameters caused by HI leads to changes in drug pharmacokinetics (PK) that may require adjustment of drug dosage. For example, the area under the plasma concentration–time curve (AUC) of a drug, primarily metabolized by the cytochrome P450 (CYP) 3A enzymes, can be increased more than 10-fold in HI versus healthy volunteers (HV).[14,15] For this reason, regulatory agencies recommend measuring drug PK in subjects with various degrees of HI (CP-A to C).[16,17] However, such PK studies are costly, time consuming, and hard to recruit into, especially subjects with CP-C. A potential solution to this dilemma is to determine the abundance of the major DMET in organs important for the absorption and disposition of drugs, namely, in the intestine, liver, and kidney, obtained from subjects with various degrees of HI.[18] With the advent of quantitative-targeted proteomics, much progress has been made in the quantification of the abundance of DMET in HI.[7,9–13] However, to use these data with confidence, such quantification needs to be validated through phenotyping PK studies in this population. Such phenotyping studies can be conducted with probe drugs of the major DMET and interpreted to reflect changes in the in vivo activity of the DMET provided the rate-determining step(s) in the CL of the drugs is (are) known.[19,20] Once validated, the DMET abundance data can be used to predict the changes in disposition in the HI of other drugs cleared by the same DMET. Although such validation for all the major DMET is logistically unrealistic, validation of a few major DMET abundance data may provide confidence in using the abundance data of the remaining DMET without the corresponding in vivo phenotyping studies.

One approach to validating DMET abundance data is through physiologically based pharmacokinetic (PBPK) models that incorporate physiological changes in HI including tissue DMET abundance as quantified by quantitative targeted proteomics.[9,10,21,22] Such models are available through widely used software such as Simcyp, GastroPlus, and PK-Sim. Therefore, here we first determined if the HI module in Simcyp simulator (Version 21), populated with CYP3A abundance data for various stages

of HI (CP-A to C) can quantitatively predict the effect of all stages of HI on the PK of CYP3A-phenotyping drugs. Then, using CYP3A drugs as an example, through simulations, we identified the salient PK factors that drive the major changes in drug exposure (AUC) in HI.

METHODS

Drug selection criteria

Eligibility criteria for the selection of CYP3A drugs and their studies in HI from the literature were as follows: (1) based on in vivo or in vitro studies, the drug must be metabolized primarily by CYP3A; (2) PK parameters (e.g., CL or AUC) of the drug after intravenous (i.v.) and/or oral (p.o.) administration must be available in the HI populations; (3) the HI population studied (e.g., CP-A, B, or C) must be specified (for some drugs, data were available for only some stages of HI); and (4) subjects with a portacaval shunt must have been excluded from the study. Based on these criteria, seven CYP3A substrates with fraction metabolized (f_m; via CYP3A) of 0.7–0.95, with low to high hepatic availability (F_H; 0.09–0.96, derived from i.v. data or predicted from Simcyp) in HV were selected, namely, alprazolam, sirolimus, nifedipine, midazolam, felodipine, buspirone, and ibrutinib (Table 1).

PBPK model development and validation for the HV population

The Simcyp simulator Version 21 (Certara) was used to predict the plasma (blood for sirolimus) PK parameters (AUC and maximum plasma/blood drug concentration [C_{max}]) and systemic (plasma or blood) concentration-time (C-T) profiles of the drugs in HV after i.v. or p.o. administration using the "HV Caucasian population" (Figure 1). The input parameters of the PBPK model were derived from compound files of the Simcyp library, the literature, or by adjusting the Simcyp library parameters to recover the observed PK profile of the drugs (Tables S1–S7). Simcyp's first-order or advanced dissolution, absorption, and metabolism model for absorption, minimal or full PBPK model for distribution, perfusion limited model for hepatic metabolism, and total renal CL model for excretion were used (Tables S1–S7). PBPK models were considered validated if the mean simulated AUC in the HV population (primary end point) fell within 0.5- to 2-fold of the observed data (twofold criterion). As a secondary end point, we also determined if the predicted C_{max} also met this criterion.

PBPK model development and validation for HI population

The Simcyp's default HI module was used to predict the drug PK profiles (i.v. or p.o.) in HI (CP-A to C) (Figure 1). The Simcyp HI model considers changes in physiology (e.g., DMET protein abundance, plasma protein binding, blood flow) in HI; the relevant selected physiological parameters for the present study are listed in Table S8. Simcyp scales the hepatic activity of CYP enzymes in HI based on changes in hepatic DMET abundance and functional liver volume. For the remaining unknown hepatic CL pathway of the drug, where abundance data are not available, Simcyp scales this hepatic activity in HI based

TABLE 1 Estimated (or predicted by Simcyp from in vitro studies) $f_{m,CYP3A}$, remainder CL pathway, F_aF_G, F_H, and fu_B of the selected CYP3A-metabolized drugs in healthy volunteers

Substrates[a]	$f_{m,CYP3A}$	Remainder CL pathway[b]	F_aF_G[c]	F_H	fu_B
Alprazolam	0.71	Hepatic (CYP3A5) and renal	0.99	0.96	0.35
Sirolimus	0.80	Hepatic (CYP3A5, CYP2C8, and unknown) and renal	0.37	0.92	0.002
Nifedipine	0.95	Hepatic (CYP3A5 and unknown)	0.74	0.62	0.05
Midazolam	0.86	Hepatic (CYP3A5 and UGT1A4) and renal	0.51	0.54	0.05
Felodipine	0.93	Hepatic (unknown)	0.45	0.38	0.005
Buspirone	0.95	Hepatic (unknown)	0.21	0.13	0.06
Ibrutinib	0.95	Hepatic (unknown) and renal	0.39	0.09	0.03

Abbreviations: CL, clearance; CYP, cytochrome P450; F_a, fraction absorbed; F_aF_G, intestinal availability; F_H, hepatic availability; $f_{m,CYP3A}$, mean fraction of drug metabolized via CYP3A; fu_B, fraction unbound in blood; UGT1A4, uridine diphosphate glucuronosyltransferase family 1, member A4.

[a]Substrates listed in the order of their F_H value.

[b]Minor drug CL pathways.

[c]F_a is assumed to be one.

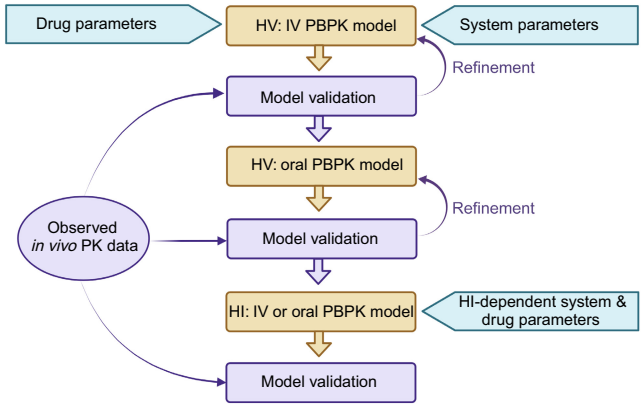

FIGURE 1 General workflow of development and validation of a PBPK model in HV (healthy volunteers) and HI (hepatically impaired) subjects. A PBPK model for each drug after intravenous and/or oral administration was developed using "HV Caucasian population" of the Simcyp simulator Version 21. The model was considered validated if the simulated PK parameters (area under the curve or maximum drug concentration) of the drug fell within 0.5- to 2-fold of the observed value. Then, the PK profiles or parameters of the drugs in the HI population after intravenous or oral administration were simulated using the default "HI population" of Simcyp Version 21. The model was considered validated if the mean ratio of the simulated PK parameters in the HI and the HV populations (ratio of the mean area under the plasma concentration–time curve or ratio of the mean maximum plasma/blood drug concentration) fell within 0.5- to 2-fold of the observed value. HV, healthy volunteer; HI, hepatic impairment; PBPK, physiologically-based pharmacokinetic; PK, pharmacokinetics.

only on the decreased functional liver volume. Simcyp scales the fraction unbound in the plasma (fu), blood-to-plasma ratio (B/P), and total renal CL in HI based on changes in drug-binding plasma protein, hematocrit, and glomerular filtration rate, respectively. For the gut availability (F_G) of the drug, Simcyp scales this in HI based on changes in the gut DMET abundance and gut villous blood flow ($Q_{B,villi}$), respectively.

For PBPK model validation, the ratio of the mean AUC and C_{max} in the HI versus HV population (AUCR and C_{max}R, respectively) were our primary and secondary PK end points, respectively. The PBPK model was considered validated if the mean simulated AUCR and C_{max}R fell within 0.5- to 2-fold range of the mean observed data. A more stringent bioequivalence criterion (0.8- to 1.25-fold) was our secondary criterion for PBPK model validation.

PBPK virtual study design

Each PBPK simulation study for the HV (Table S9) and the HI population (Table S10) was conducted with 20 virtual trials with the same number of subjects, age range, sex distribution, and dosing regimen as the corresponding in vivo PK study.

Identification of factors that affect the PK of CYP3A drugs in HI after i.v. or p.o. drug administration

Using PK principles, the PK factors driving the increase in blood AUCR of CYP3A-metabolized drugs were determined using virtual drugs following i.v. or p.o. drug administration. The drugs were assumed to be acidic, bound only to human serum albumin, and to have a B/P equal to 0.60.[23,24]

i.v. administration

The drugs were assumed to be metabolized in HV by hepatic CYP3A (f_m, 0.95; based on CYP3A probe drug data) and the remaining pathway (f_m, 0.05) was assigned to CYP2C9 enzymes, as it is often a pathway that also metabolizes CYP3A drugs.[25] They were categorized into three groups based on their low (0.15), medium (0.5), or high (0.85) F_H or fraction unbound in the blood (fu_B) in HV. The hepatic well-stirred model was used to simulate blood AUC values for HV and HI (CP-A to C) populations as well as the AUCR (ratio of AUC in HI to that in HV), after i.v. administration of the CYP3A drug, using the Simcyp HV and HI populations (Equation 1).[26,27]

$$\frac{AUC_{IV}}{Dose} = \frac{1}{CL_{B,H}} = \frac{Q_{B,H} + fu_B \bullet CL_{int,H}}{Q_{B,H} \bullet fu_B \bullet CL_{int,H}} \quad (1)$$

where $CL_{B,H}$, $Q_{B,H}$, fu_B, $CL_{int,H}$, and AUC_{IV} represent in vivo hepatic blood CL, hepatic blood flow, fraction unbound in the blood, in vivo hepatic intrinsic CL, and area under the blood drug C-T curve after i.v. administration, respectively. The $CL_{int,H}$ in HV was back calculated using the hepatic well-stirred model (Equation 2). $CL_{int,H}$, fraction unbound in the plasma, and B/P were scaled in HI using total molar hepatic DMET abundance protein, drug-binding plasma protein, and hematocrit, respectively.[21,28–31]

$$F_H = \frac{Q_{B,H}}{Q_{B,H} + fu_B \bullet CL_{int,H}} \quad (2)$$

where F_H represents hepatic availability.

p.o. administration

The drugs were assumed to be metabolized in HV by intestinal CYP3A (f_m, 0.95) and CYP2C9 (f_m, 0.05; in the

intestine, CYP2C9 is the second most expressed CYP enzyme after CYP3A[32]) with no other elimination pathways. The corresponding hepatic f_m as well as the total $CL_{int,H}$ were calculated using the total molar DMET protein abundance in the liver relative to that in the gut. The drugs were categorized into three groups based on their low (0.15), medium (0.5), or high (0.85) intestinal availability (F_aF_G) or fu_B in HV. The drugs were assumed to be highly permeable across the gut wall (fraction absorbed, 1; as the majority of selected CYP3A probe drugs have an n-octanol/water partition coefficient of >2.5), with a fraction unbound in the gut of unity (fu_G; the gut effective flow model improved the gut availability prediction when fu_G was assumed to be 1[33]). Blood AUC values for HV and HI (CP-A to C) populations as well as the AUCR (ratio of AUC in HI to that in HV) after p.o. administration of the CYP3A drug were simulated using the gut effective flow (commonly known as Q_{Gut}) model and Simcyp HV and HI populations (Equation 3).[27,33]

$$\frac{AUC_{PO}}{Dose} = \frac{F}{CL_{B,H}} = \frac{F_a \bullet F_G \bullet F_H}{CL_{B,H}} = \frac{F_a \bullet F_G}{fu_B \bullet CL_{int,H}} \quad (3)$$

where

$$F_G = \frac{Q_{Gut}}{Q_{Gut} + fu_G \bullet CL_{int,G}} \quad (4)$$

F, F_a, F_G, Q_{Gut}, fu_G, $CL_{int,G}$, and AUC_{PO} represent oral bioavailability, fraction absorbed, gut or intestinal availability, gut hybrid flow term includes both permeability through the enterocyte membrane (CL_{perm}) and $Q_{B,villi}$, fraction unbound in the gut, in vivo gut intrinsic CL, and area under the blood drug C-T curve after p.o. administration, respectively. $CL_{int,G}$ was back calculated using the gut effective flow model (Equation 4). $CL_{int,G}$ or $CL_{int,H}$ and fu_B were scaled in HI using total molar DMET abundance protein in the liver or gut and drug-binding plasma protein, respectively. For highly permeable drugs, Q_{Gut} was assumed to be equivalent to $Q_{B,villi}$ using Equation (5).

$$Q_{Gut} = \frac{Q_{B,villi} \bullet CL_{perm}}{Q_{B,villi} + CL_{perm}} \quad (5)$$

where Q_{Gut}, $Q_{B,villi}$, and CL_{perm} represent gut hybrid flow term, gut villous blood flow, and a CL term defining permeability through the enterocyte, respectively.

For both i.v. and p.o. administration, average virtual Simcyp HV and HI populations were generated from 20 virtual trials consisting of 10 human subjects (50% female), 18 to 65 years of age (Table S11).

RESULTS

Comparison of the PBPK model-simulated and observed systemic concentration of drugs in HV after i.v. or p.o. administration

Simulated mean plasma (blood for sirolimus) C-T profiles of all CYP3A substrates after i.v. or p.o. drug administration published by others were successfully reproduced. Mean observed C-T profiles of all drugs fell within the 5th and 95th percentiles of the simulated data (Figure 2). The ratio of the simulated and observed PK parameters (AUC or C_{max}) values for all drugs passed our a priori set twofold acceptance criterion (Table S12).

Comparison of the PBPK model-predicted and observed systemic concentration of drugs (i.v. or p.o.) in people with HI

The default physiological parameters of the HI populations of the Simcyp's HI module successfully predicted the PK of the CYP3A drugs in HI (CP-A to C). The ratio of the simulated and observed AUCR values of the drugs (i.v. and p.o., $n = 17$ studies) for all stages of HI fell within our a priori defined twofold acceptance criterion (Figures 3 and 4; Table S13). Similarly, the model-predicted C_{max}R of the drugs fell within our a priori twofold acceptance criterion (Table S13). In addition, 53% of the AUCR and 56% of the C_{max}R of the 15 and nine studies, respectively, fell within our more stringent bioequivalence criterion (Figure 4).

Factors that affect the PK of CYP3A drugs in HI after i.v. administration

Blood AUCR was modestly affected by HI and was larger for drugs with high F_H versus those with low or medium F_H, as revealed by the simulations. In addition, the AUCR was larger for drugs with high fu_B versus those with low or medium fu_B (Figure 5).

Factors that affect the PK of CYP3A drugs in HI after p.o. administration

Blood AUCR of drugs in HI was larger for drugs with low F_aF_G versus those with medium or high F_aF_G, as revealed by the simulations. In addition, AUCR was larger for

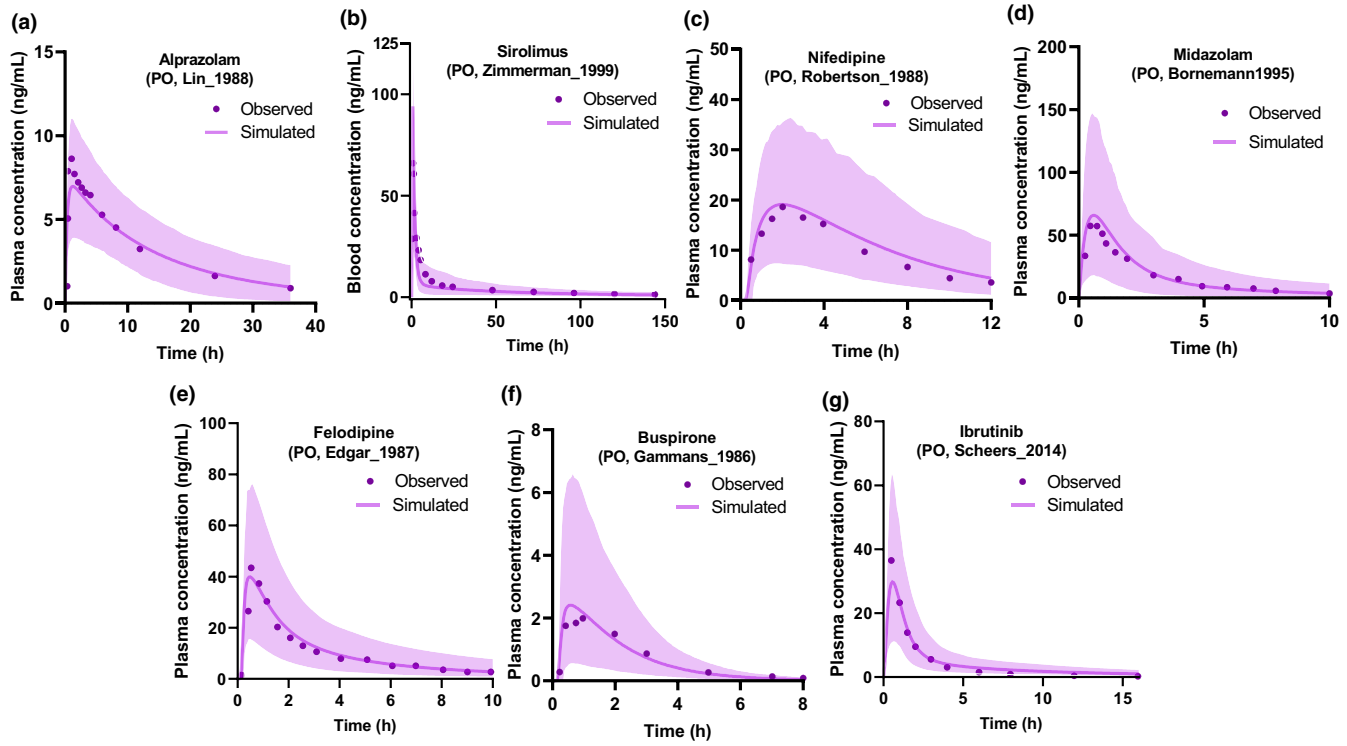

FIGURE 2 Simulated and observed mean plasma (for sirolimus, blood) concentration–time profiles of (a) alprazolam, (b) sirolimus, (c) nifedipine, (d) midazolam, (e) felodipine, (f) buspirone, and (g) ibrutinib in healthy volunteers after oral (PO) administration. The observed mean drug concentration–time data (filled circles) were in excellent agreement with the mean simulated data (continuous line) and fell within the 5th and 95th percentiles (shaded areas) of the simulated data. The predicted pharmacokinetic parameters (area under the curve and maximum drug concentration) also fell within 0.5- to 2-fold of the observed values (Table S12). Each simulation was conducted with 20 virtual trials with the same number of subjects, age range, sex distribution, and dosing regimen of the relevant pharmacokinetics study (Table S9).

drugs with high fu_B versus those with low or medium fu_B (Figure 6).

DISCUSSION

Numerous studies evaluating the prediction of changes in drug PK due to HI using PBPK models have been published,[28,29,34] but none have focused on validating the changes in the PK of multiple probe substrates of a given DMET. Therefore, it is not possible to use the findings of these studies to generalize beyond the drugs studied. To the best of our knowledge, this is the first study to comprehensively address whether disposition of CYP3A probe drugs in patients with HI can be predicted using a PBPK model populated with hepatic and intestinal CYP3A abundance data.

We chose to study CYP3A enzymes as they are involved in metabolism of more than 50% of the approved drugs cleared by CYP metabolism.[35] From these drugs, we chose drugs that are predominantly metabolized by CYP3A enzymes ($f_m > 0.70$) but have varying degrees of F_G (0.21–0.99) and F_H (0.09–0.96). The drugs were chosen to have minimal or negligible biliary or renal elimination of parent drug with little to no known involvement of transporters to ensure that CYP3A-mediated metabolism is the primary and rate-determining pathway in their CL. In addition, prediction of the disposition of these drugs in HI was performed with the most up-to-date version of Simcyp (Version 21) using the drug's validated PBPK data files from the Simcyp library or those published in the literature. The version of Simcyp used is populated with hepatic CYP activity or abundance data for HV as well as with those with HI (Table S8).[36]

In the absence of recommended guidelines for model acceptance criteria, we set the conventional, widely used, twofold boundary as our primary validation criterion and the more stringent bioequivalence (1.25-fold) boundary as our secondary validation criterion.[37] The latter is important when recommending dose adjustment. We chose the mean AUCR as the primary end point because our main goal was to obtain comparable drug exposure in HV and subjects with HI. In addition, we selected the mean drug C_{max}R as our secondary end point because C_{max} is often related to drug safety and/or efficacy.

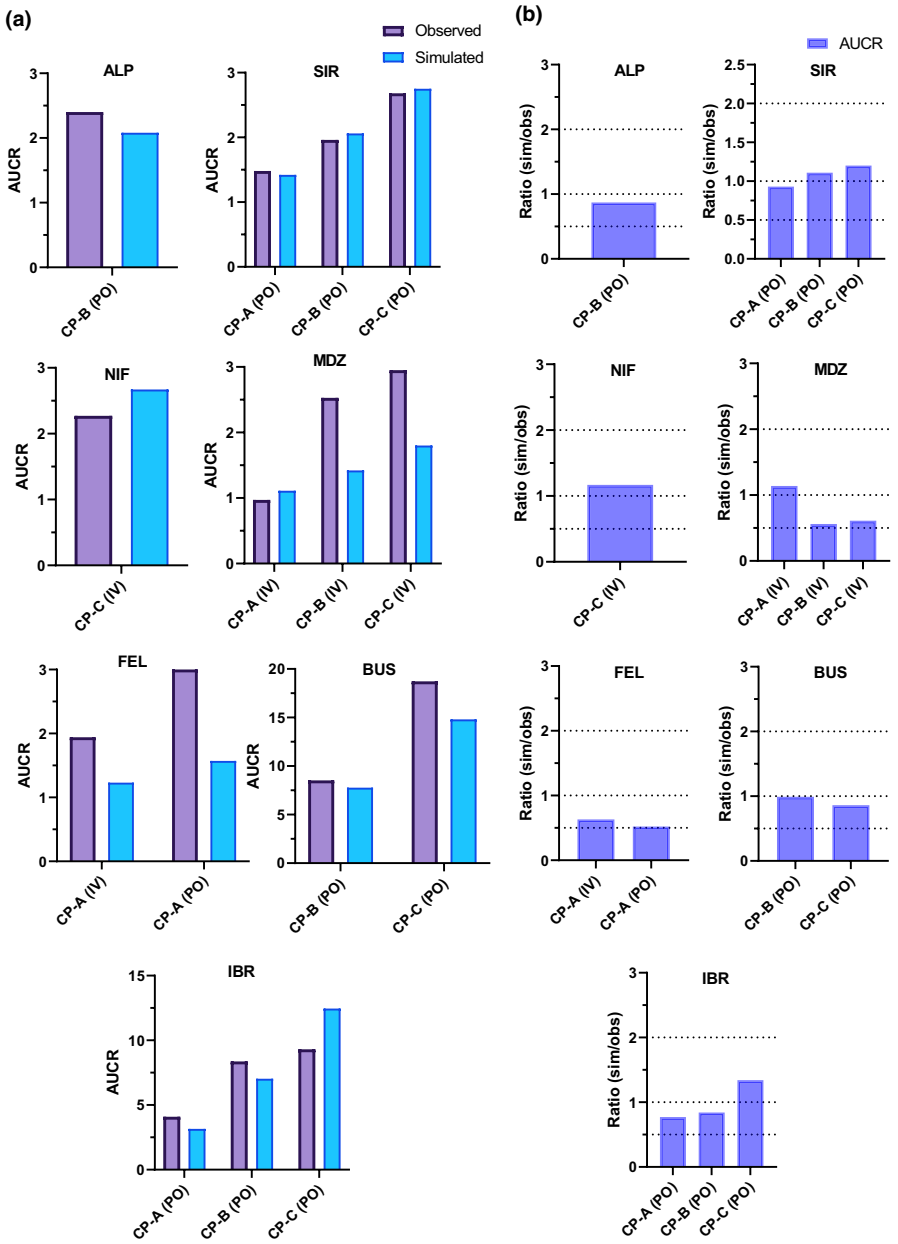

FIGURE 3 Predictive performance of the physiologically-based pharmacokinetic model, for each cytochrome P450 (CYP) 3A drug, for different stages of hepatic impairment (HI). Observed versus simulated mean value of the drug AUCR (i.e., ratio of the area under the curve in HI and healthy volunteers) (a) and the ratio of the simulated and the observed AUCR (b). The simulated AUCR is in good agreement with the observed AUCR for all seven CYP3A drug and all stages of HI. The ratio of the simulated (sim) and observed (obs) values (AUCR or C_{max}R) fell within a priori defined acceptance criterion (0.5–2) (Table S13). Each simulation was conducted with 20 virtual trials with the same number of subjects, age range, sex distribution, and dosing regimen of the relevant pharmacokinetics study (Table S10). *Note*: For some drugs, literature data were not available for all stages of HI. ALP, alprazolam; AUCR, ratio of the mean area under the plasma (blood for sirolimus) concentration–time curve ; BUS, buspirone; C_{max}R, ratio of the mean maximum plasma/blood drug concentration; CP, Child–Pugh; FEL, felodipine; IBR, ibrutinib; IV, intravenous; MDZ, midazolam; NIF, nifedipine; PO, oral; SIR, sirolimus.

Before analyzing the performance of the PBPK model to predict disposition of CYP3A drugs in HI, we confirmed that the model adequately predicted (within a priori set acceptance criterion) the PK of all the drugs in HV (after i.v. and p.o. administration). On visual inspection, the observed C-T profiles of drugs in HV fell between the 5th and 95th percentiles of the predicted mean values (only p.o. data are shown in Figure 2). Consequently, the predicted PK parameters (AUC and C_{max}) of all the drugs also fell within 0.5- to 2-fold of the observed values (Table S13). However, not all the predictions met our more stringent 1.25-fold criterion, but there were no discernible characteristics of those drugs that did not meet this criterion (Figures 3 and 4). We speculate that this difference could be due to different interindividual variability in the PK studies compounded by the etiology of the disease and small sample size. Most of the listed studies followed regulatory guidelines and studied mostly 6–18 subjects.[6,17] An additional explanation is that CP scores do not adequately capture disease-dependent variability in physiological changes (e.g., expression of DMET is dependent on the etiology of the disease).[6] Collectively, these factors may make it challenging, if not impossible, to meet the bioequivalence criterion for predicting other phenotyping drug studies conducted in people with HI.

To dissect factors that drive the changes in disposition of CYP3A-metabolized drugs in HI, we conducted simulation studies. A key assumption we made is the drug in question had an f_m via hepatic or intestinal CYP3A enzymes of 0.95, with the remainder pathway (f_m =0.05) being CYP2C9. This assumption is key because the largest change in AUCR will be for those drugs that are

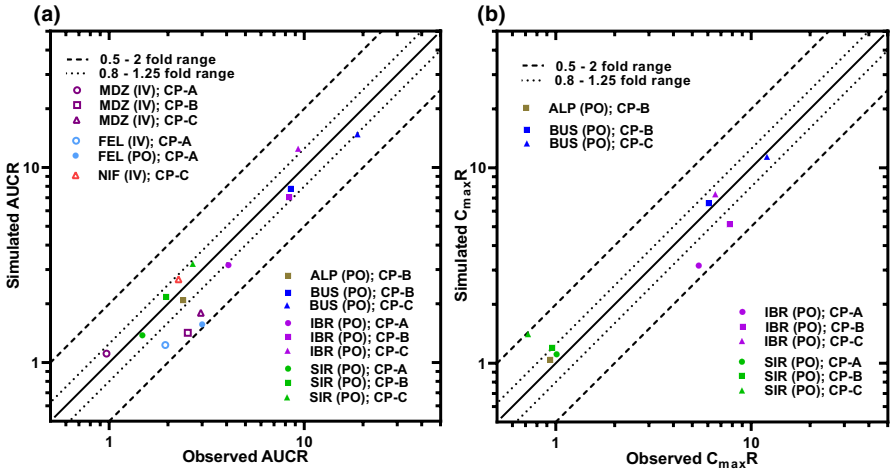

FIGURE 4 Plots to illustrate the performance of the physiologically-based pharmacokinetic model for the seven cytochrome P450 3A drugs at different stages of hepatic impairment. The simulated (a) AUCR or (b) C_{max}R for all drugs fell within 0.5- to 2-fold of the observed value (Table S13). AUCR and C_{max}R are, respectively, the mean ratio (hepatic impairment/healthy volunteers) of the simulated and observed drug AUC and C_{max}. Dashed, dotted, and solid continuous lines denote the 0.5- to 2-fold range, 0.8- to 1.25-fold range, and unity, respectively. Open and closed symbols represent pharmacokinetic parameters after intravenous and oral administration, respectively. Circles, squares, and triangles represent pharmacokinetic parameters for CP scores A–C, respectively. ALP, alprazolam; AUC, area under the plasma (blood for sirolimus) concentration–time curve; BUS, buspirone; C_{max}, maximum plasma (blood for sirolimus) concentration; CP, Child–Pugh; FEL, felodipine; IBR, ibrutinib; IV, intravenous; MDZ, midazolam; NIF, nifedipine; PO, oral; SIR, sirolimus.

predominately metabolized (or transported) via the pathway(s) that is significantly affected by HI. For drugs administered orally, the hepatic f_m and CL of the drug were scaled based on the relative abundance of the enzymes in the liver versus the intestine.

Our simulations revealed that, for i.v. administration of the CYP3A drugs, the blood AUCR increases with an increase in F_H and fu_B, and, as expected, with severity of HI (Figure 5). This is because the hepatic CL of drugs with low F_H (high hepatic extraction) will be mostly dependent on $Q_{B,H}$ rather than CYP3A-mediated intrinsic CL, and the change in $Q_{B,H}$ in HI is small relative to the change in hepatic CYP3A abundance (Table S11[36]). It is worth mentioning that as CYP3A abundance in the liver decreases (80%) with increased severity of HI, the hepatic CL of drugs with low F_H will become sensitive to both $Q_{B,H}$ and CYP3A-mediated intrinsic CL because it will transition from a low F_H to a mid F_H drug. Also, this is relevant for drug–drug interaction (DDI), where the magnitude of the DDI can increase due to HI.

In contrast to high hepatic extraction drugs, the hepatic CL of drugs with high F_H is mostly dependent on the intrinsic CL (CL_{int}) via CYP3A (and not $Q_{B,H}$) and therefore most affected by changes in hepatic CYP3A abundance caused by HI. Similarly, the total CL of drugs with high fu_B is directly related to hepatic CYP3A abundance (and CL_{int}), whereas those with low fu_B are dependent on both CYP3A abundance and drug-binding plasma protein concentration. Consequently, decreased serum albumin and hepatic CYP3A abundance in HI results in an increase in fu_B and a decrease in $CL_{int,H}$ in HI, which can counteract each other's effect on the magnitude of change in the hepatic (total) CL of drugs. However, it is important to recognize that changes in fu_B alone for high F_H (without a concomitant change in $CL_{int,H}$) will result in change in total CL of the drug and will be reflected in the drug AUC based on total plasma concentrations. But, at the same time, the unbound drug plasma AUC will be unchanged provided $CL_{int,H}$ is unchanged.[27,38] Because it is the unbound drug that is pharmacologically active, this discordance should be kept in mind when considering dose adjustment. Alternatively stated, this dependency on fu_B (without a concomitant change in $CL_{int,H}$) will disappear if the unbound CL (or unbound AUCR) of the drug is computed. In this case, no adjustment in dose would be needed. Collectively, the effect of HI on AUCR of CYP3A-metabolized drugs administered i.v. is modest compared with its effect on drugs administered orally (see next paragraph).

For oral drug administration, our simulations revealed that the effect of HI on AUCR of CYP3A drugs increased as the magnitude of the drug's F_aF_G decreased and as fu_B increased. This is because AUCR for low F_aF_G is determined by $Q_{B,villi}$, $CL_{int,G}$, fu_B, and $CL_{int,H}$ parameters. As CYP3A abundance in the intestine and the liver decreases with increased severity of HI, the first-pass extraction of the drugs by these organs decreases, resulting in F_aF_G to increase toward unity (we assumed F_a did not change in HI). A low F_aF_G (due to intestinal metabolism) also means a low F_H. Therefore, as F_aF_G increases

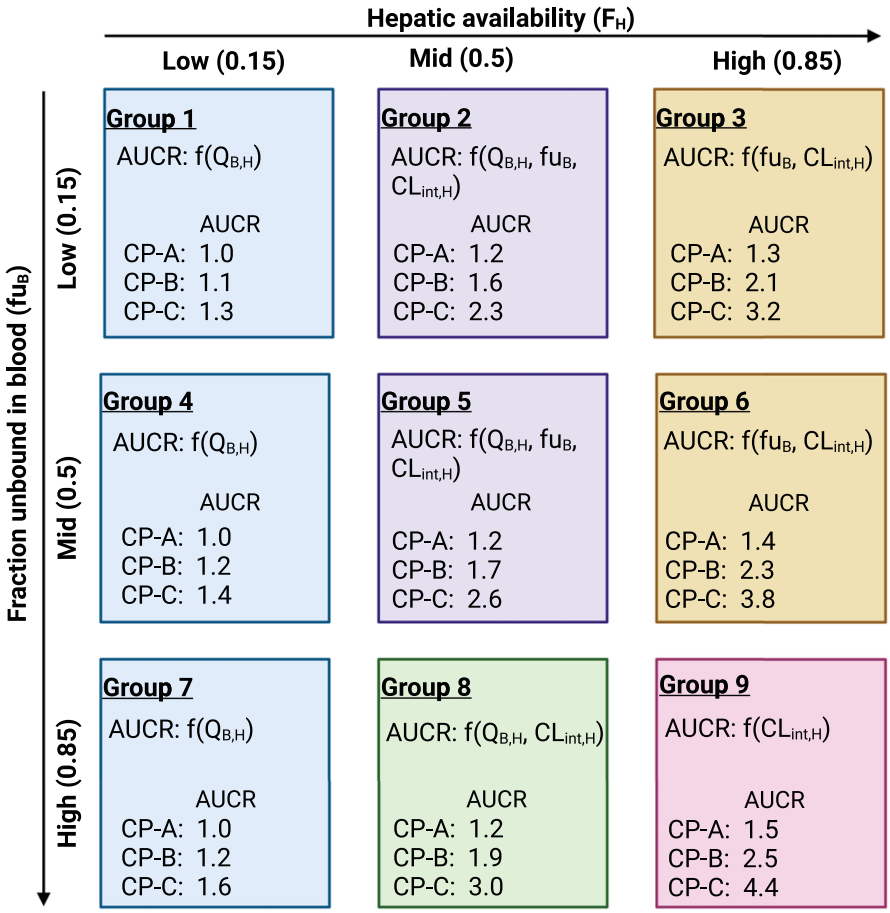

FIGURE 5 Factors that affect the AUCR of cytochrome P450 (CYP) 3A drugs in hepatic impairment (Child–Pugh [CP] score A–C) after intravenous administration. The CYP3A-metabolized drugs (fraction metabolized, 0.95) were categorized into three groups by their hepatic availability (F_H) and fraction unbound in the blood (fu_B): 0.15 (low), 0.5 (medium), and 0.85 (high). The groups are color coded depending on the factors that affect their AUCR (listed as *f*[*x*,*y*,*z*]). The magnitude of change in AUCR caused by hepatic impairment increased as F_H and fu_B increased. The well-stirred hepatic clearance model was used to simulate blood AUCR values using the Simcyp Version 21 hepatic impairment module (Table S11). Drugs were assumed to be primarily metabolized by CYP3A and 2C9 enzymes, with the fraction metabolized in healthy volunteers equal to 0.95 and 0.05, respectively, bound only to human serum albumin and with no renal clearance. AUCR, ratio of the mean area under the plasma concentration–time curve; $CL_{int,H}$, hepatic intrinsic clearance; $Q_{B,H}$, hepatic blood flow.

toward unity, F_H also increases toward unity, but this time due to a reduction in hepatic CYP3A abundance. Collectively, this results in a large change in overall bioavailability in HI and therefore AUCR. This is likely to be true for drugs metabolized by both hepatic and intestinal drug-metabolizing enzymes, such as CYP3A and CYP2C9. Of note, as expected, the AUC of drugs with high F_aF_G is determined by $CL_{int,H}$ (and therefore F_H) and fu_B (when fu_B is low or medium) (Groups 3, 6, and 9). Therefore, as was the case for i.v. administration, the effect of HI on drug AUC is modest.

Similar to i.v. administration, the AUCR for a high fu_B drug given orally is mostly dependent on $Q_{B,villi}$, $CL_{int,G}$, and $CL_{int,H}$ and less so on fu_B. However, we should note here that for drugs that are extensively metabolized in the liver, fu_B rarely, if ever, falls in the high category. High fu_B drugs are usually eliminated via renal CL and not hepatic metabolism.[39,40] To illustrate, the highest fu_B observed among our CYP3A probe drugs is 0.35 for alprazolam (Table 1). And, for such drugs, F_aF_G and F_H will be high and therefore their AUC will be less affected by HI. This is because the gut availability of such drugs is close to unity and the AUCR is driven primarily by hepatic CL_{int} and less so by fu_B. For example, alprazolam is primary metabolized by CYP3A enzymes (f_m, 0.71) with high F_aF_G (~0.99), high F_H (0.96), and moderate fu_B (0.35). In subjects with moderate HI (CP-B), the AUCR of alprazolam was only modestly affected (2.1; Simcyp simulated). In practice, extensively metabolized drugs will likely fall in the mid to low fu_B range in Figure 6. For example, buspirone is extensively metabolized by CYP3A enzymes (f_m, 0.95) with low F_aF_G (=0.21), low F_H (0.13), and low fu_B (0.06). Patients with severe HI had a plasma buspirone AUCR of ~15 (Simcyp simulated) because in HI, F_aF_G increased to

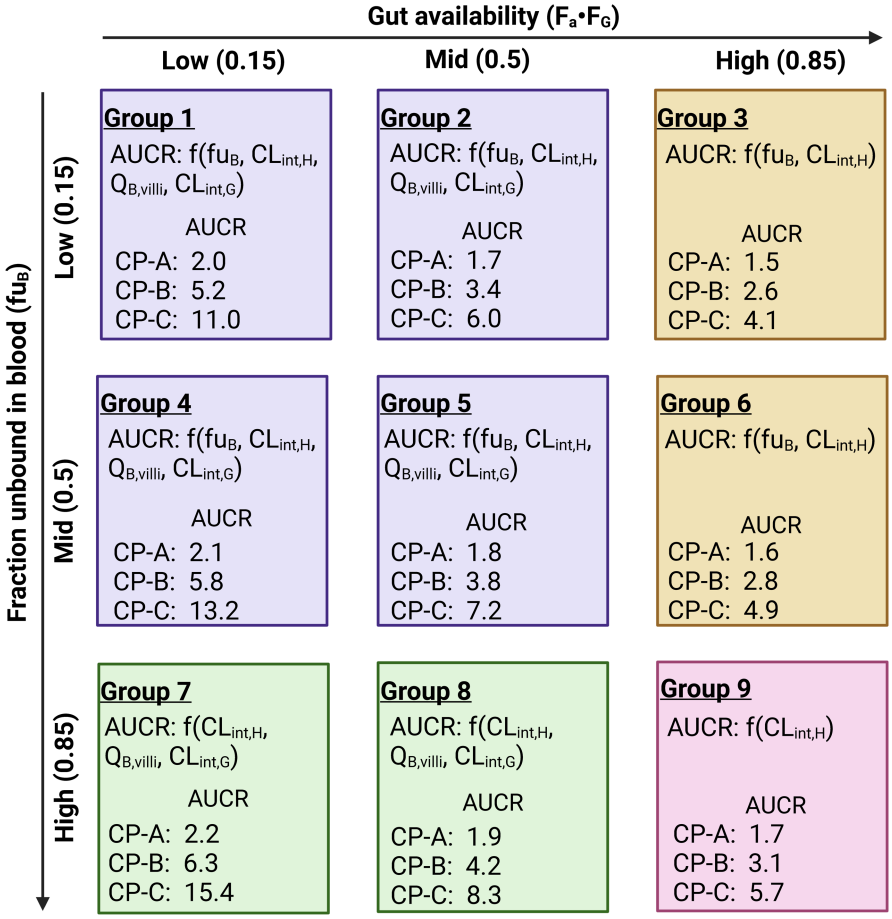

FIGURE 6 Factors that affect the AUCR of cytochrome P450 (CYP) 3A drugs in hepatic impairment (Child–Pugh [CP] score A-C) after oral administration. The CYP3A-metabolized drugs (fraction metabolized [f_m], 0.95 in the intestine) were categorized into three groups by their gut availability (F_aF_G) and fraction unbound in the blood (fu_B): 0.15 (low), 0.5 (medium), and 0.85 (high). The groups are color coded depending on factors that affect their AUCR (listed as f[*x*,*y*,*z*]). The magnitude of change in AUCR caused by hepatic impairment increased as F_aF_G decreased and fu_B increased. The well-stirred hepatic and effective flow gut models were used to simulate blood AUCR values using the Simcyp Version 21 hepatic impairment module (Table S11). Drugs were assumed to be primarily metabolized by CYP3A and CYP2C9 enzymes, with intestinal f_m in healthy volunteers equal to 0.95 and 0.05, respectively, bound only to human serum albumin, with no renal clearance, high fraction absorbed ($F_a = 1$), and no binding to intestinal tissue ($fu_G = 1$). The corresponding f_m and total CL_{int} in the liver were calculated based on the abundance of CYP3A and CYP2C9 in the liver versus the intestine. AUCR, ratio of the mean area under the plasma concentration–time curve; CL_{int}, intrinsic clearance; $CL_{int,G}$, gut intrinsic clearance; $CL_{int,H}$, hepatic intrinsic clearance; F_a, fraction absorbed; fu_G, fraction unbound in the gut; $Q_{B,villi}$, gut villous blood flow.

0.75 (calculated using Equation 3), F_H increased to 0.33, and fu_B increased to 0.12. As elaborated for i.v. administration, in the absence of a change in $CL_{int,H}$, although the drug AUC based on total plasma concentration will be affected by changes in fu_B, the unbound AUC will be unaffected. But, in contrast to i.v. administration, this will be the case for all F_H values.[27,38] Therefore, in this case, dose adjustment would be unnecessary.

Although the aforementioned simulations (for i.v. and p.o. administrations) were conducted using CYP3A-metabolized drugs, the factors that drive the change in the PK of drugs in HI are independent of the DMET involved. Thus, the results of our simulation studies can be generalized to other drugs that are primarily metabolized (or transported) by other enzymes (or transporters). That is, for orally administered drugs, extensively metabolized or transported in the intestine (e.g., effluxed by P-glycoprotein [P-gp]) and/or the liver, the factors that will result in large AUCR in HI are low F_H and low F_aF_G.

There are a few limitations to our work. First, data on regional intestinal abundances of DMET in cirrhosis due to different etiology has not been well characterized, which can affect drugs extensively metabolized/transported in the intestine. Second, i.v. data are not available for many drugs to verify liver versus gut contribution in drug disposition. Third, a drug's F_a can be dependent on intestinal permeability, bile salt concentration, and expression of membrane transporters, all of which might be

affected by HI; however, these factors have not been well characterized in HI.[41,42] Fourth, we assumed that reduced protein abundance in HI translates into lower enzyme activity as the latter was not measured. Fifth, a few reports suggest that P-gp could also be involved in sirolimus disposition. Interestingly, the oral PK of a P-gp probe drug, dabigatran etexilate, are not affected in moderate HI, suggesting no impact of HI on intestinal P-gp activity.[43]

In summary, the Simcyp Version 21 default HI PBPK model can predict, within twofold of the observed data, the PK of CYP3A substrate drugs at different stages of HI. This level of accuracy is unlikely to be sufficient for regulatory agencies to allow the prediction of dosing regimens of narrow therapeutic window CYP3A drugs, for people with HI, without conducting PK studies in this population. In contrast, this level of accuracy may be sufficient to obtain such a waiver for drugs with a wide therapeutic window. Of course, the drug in question would also need to be extensively metabolized by CYP3A enzymes in HV. Alternatively, irrespective of the size of the therapeutic window of the CYP3A drug, this PBPK model could be used to design PK studies of such drugs for CP-A and CP-B subjects that are easier to recruit. Then, if the model can accurately predict the PK of the drug in question in these populations, regulatory agencies may be willing to allow dosing recommendations for CP-C subjects without conducting PK studies in that population. To successfully extend this strategy to drugs predominately metabolized/transported by other DMET or DMET in combination, the HI PBPK model will need to be validated by conducting phenotyping studies for other DMET in HI. Although it is unrealistic and logistically impossible to conduct such phenotyping studies for all DMET, they could be conducted for the major DMET. Then, validation of the model using such studies, in combination with DMET abundance in the liver, intestine, and kidneys, could be used in the future to predict dosing regimens of drugs for people with HI without conducting PK studies in this population. In this regard, it is critical that quantification of DMET abundance in these tissues, obtained from subjects with HI, be conducted. It would be best if such tissues were available from subjects with known etiology of HI as the etiology can have a differential effect on the abundance (and therefore activity) of the DMET.[9] Also, it is important to explore classification methods, other than CP scores, for categorizing the severity of HI that better reflects the impact of HI on DMET activity and abundance.

Our simulations also identified PK factors (F_aF_G, F_H, and fu_B) that can drive the large increase in the blood AUC of drugs that are extensively metabolized by CYP3A enzymes after i.v. and p.o. administration. Although our simulations focused on CYP3A substrate drugs, the factors elucidated can be applied to any DMET. Thus, these learnings could be used in the future to determine the likely magnitude of HI on the PK of a drug in question. It is important to note here that fu_B impacts only the total and not the unbound concentrations of the drug; the latter drives the efficacy and safety of drugs. Thus, adjusting dosing based on the determination of total drug AUC in HI would be incorrect. Instead, such dosing adjustments should be based on changes, if any, in the unbound AUC of the drug.

AUTHOR CONTRIBUTIONS

M.K.L., F.S., X.L., Y.L., O.J.E., P.P.C., R.E., and J.D.U. wrote the manuscript. M.K.L., F.S., X.L., Y.L., O.J.E., P.P.C., R.E., and J.D.U. designed the research. M.K.L. performed the research. M.K.L., F.S., and J.D.U. analyzed the data.

ACKNOWLEDGMENTS

The authors thank members of the Unadkat laboratory for their valuable suggestions on the article. Servier Medical Art (https://smart.servier.com/), BioRender (https://biorender.com/), and Microsoft Office Excel and PowerPoint (https://www.office.com/) were used to create the figures.

FUNDING INFORMATION

The study was supported by the University of Washington Research Affiliate Program on Transporters funded by Amgen, Gilead, Janssen Pharmaceuticals, and Takeda Pharmaceuticals U.S.A.

CONFLICT OF INTEREST

X.L., Y.L., O.J.E., P.P.C., and R.E. are employees of their respective companies and receive stocks or stock options from their companies. All other authors declared no competing interests for this work.

ORCID

Mayur K. Ladumor https://orcid.org/0000-0003-2632-8525
Yurong Lai https://orcid.org/0000-0001-9505-333X

REFERENCES

1. Cheemerla S, Balakrishnan M. Global epidemiology of chronic liver disease. *Clin Liver Dis*. 2021;17:365-370.
2. Child CG, Turcotte JG. Surgery and portal hypertension. *Major Probl Clin Surg*. 1964;1:1-85.
3. Pugh RN, Murray-Lyon IM, Dawson JL, Pietroni MC, Williams R. Transection of the oesophagus for bleeding oesophageal varices. *Br J Surg*. 1973;60:646-649.
4. Schuppan D, Afdhal NH. Liver cirrhosis. *Lancet*. 2008;371:838-851.
5. Sharma S, Suresh Ahire D, Prasad B. Utility of quantitative proteomics for enhancing the predictive ability of physiologically based pharmacokinetic models across disease states. *J Clin Pharmacol*. 2020;60(Suppl 1):S17-S35.

6. El-Khateeb E, Darwich AS, Achour B, Athwal V, Rostami-Hodjegan A. Review article: Time to revisit Child-Pugh score as the basis for predicting drug clearance in hepatic impairment. *Aliment Pharmacol Ther*. 2021;54:388-401.
7. Chu X, Prasad B, Neuhoff S, et al. Clinical implications of altered drug transporter abundance/function and PBPK modeling in specific populations: an ITC perspective. *Clin Pharmacol Ther*. 2022;112:501-526.
8. Murphy WA, Adiwidjaja J, Sjöstedt N, et al. Considerations for physiologically based modeling in liver disease: from nonalcoholic fatty liver (NAFL) to nonalcoholic steatohepatitis (NASH). *Clin Pharmacol Ther*. 2022;1-23. doi:10.1002/cpt.2614
9. Wang L, Collins C, Kelly EJ, et al. Transporter expression in liver tissue from subjects with alcoholic or hepatitis C cirrhosis quantified by targeted quantitative proteomics. *Drug Metab Dispos*. 2016;44:1752-1758.
10. Prasad B, Bhatt DK, Johnson K, et al. Abundance of phase 1 and 2 drug-metabolizing enzymes in alcoholic and hepatitis C cirrhotic livers: a quantitative targeted proteomics study. *Drug Metab Dispos*. 2018;46:943-952.
11. El-Khateeb E, Achour B, Al-Majdoub ZM, Barber J, Rostami-Hodjegan A. Non-uniformity of changes in drug-metabolizing enzymes and transporters in liver cirrhosis: implications for drug dosage adjustment. *Mol Pharm*. 2021;18:3563-3577.
12. Drozdzik M, Lapczuk-Romanska J, Wenzel C, et al. Gene expression and protein abundance of hepatic drug metabolizing enzymes in liver pathology. *Pharmaceutics*. 2021;13:1334.
13. Drozdzik M, Szelag-Pieniek S, Post M, et al. Protein abundance of hepatic drug transporters in patients with different forms of liver damage. *Clin Pharmacol Ther*. 2020;107:1138-1148.
14. Barbhaiya RH, Shukla UA, Pfeffer M, et al. Disposition kinetics of buspirone in patients with renal or hepatic impairment after administration of single and multiple doses. *Eur J Clin Pharmacol*. 1994;46:41-47.
15. Jong J d et al. Single-dose pharmacokinetics of ibrutinib in subjects with varying degrees of hepatic impairment. *Leuk Lymphoma*. 2017;58:185-194.
16. EMA evaluation of the pharmacokinetics medicinal products in patients with impaired hepatic function. European Medicines Agency. 2018. https://www.ema.europa.eu/en/evaluation-pharmacokinetics-medicinal-products-patients-impaired-hepatic-function
17. US FDA, C. for D. E. and pharmacokinetics in patients with impaired hepatic function: study design, data analysis, and impact on dosing and labeling. US Food and Drug Administration. 2020. https://www.fda.gov/regulatory-information/search-fda-guidance-documents/pharmacokinetics-patients-impaired-hepatic-function-study-design-data-analysis-and-impact-dosing-and
18. Ahire D, Kruger L, Sharma S, Mettu VS, Basit A, Prasad B. Quantitative proteomics in translational absorption, distribution, metabolism, and excretion and precision medicine. *Pharmacol Rev*. 2022;74:769-796.
19. Patilea-Vrana G, Unadkat JD. Transport vs. Metabolism: what determines the pharmacokinetics and pharmacodynamics of drugs? Insights from the extended clearance model. *Clin Pharmacol Ther*. 2016;100:413-418.
20. Storelli F, Yin M, Kumar AR, et al. The next frontier in ADME science: predicting transporter-based drug disposition, tissue concentrations and drug-drug interactions in humans. *Pharmacol Ther*. 2022;238:108271.
21. Ladumor MK, Thakur A, Sharma S, et al. A repository of protein abundance data of drug metabolizing enzymes and transporters for applications in physiologically based pharmacokinetic (PBPK) modelling and simulation. *Sci Rep*. 2019;9:9709.
22. Vildhede A, Kimoto E, Pelis RM, Rodrigues AD, Varma MVS. Quantitative proteomics and mechanistic modeling of transporter-mediated disposition in nonalcoholic fatty liver disease. *Clin Pharmacol Ther*. 2020;107:1128-1137.
23. Riley RJ, McGinnity DF, Austin RP. A unified model for predicting human hepatic, metabolic clearance from in vitro intrinsic clearance data in hepatocytes and microsomes. *Drug Metab Dispos Biol Fate Chem*. 2005;33:1304-1311.
24. Sohlenius-Sternbeck A-K, Afzelius L, Prusis P, et al. Evaluation of the human prediction of clearance from hepatocyte and microsome intrinsic clearance for 52 drug compounds. *Xenobiotica Fate Foreign Compd Biol Syst*. 2010;40:637-649.
25. Subramanian M, Tam H, Zheng H, Tracy TS. CYP2C9-CYP3A4 protein-protein interactions: role of the hydrophobic N terminus. *Drug Metab Dispos*. 2010;38:1003-1009.
26. Pang KS, Han YR, Noh K, Lee PI, Rowland M. Hepatic clearance concepts and misconceptions: why the well-stirred model is still used even though it is not physiologic reality? *Biochem Pharmacol*. 2019;169:113596.
27. Benet LZ, Hoener B. Changes in plasma protein binding have little clinical relevance. *Clin Pharmacol Ther*. 2002;71:115-121.
28. Edginton AN, Willmann S. Physiology-based simulations of a pathological condition: prediction of pharmacokinetics in patients with liver cirrhosis. *Clin Pharmacokinet*. 2008;47:743-752.
29. Johnson TN, Boussery K, Rowland-Yeo K, Tucker GT, Rostami-Hodjegan A. A semi-mechanistic model to predict the effects of liver cirrhosis on drug clearance. *Clin Pharmacokinet*. 2010;49:189-206.
30. Salem F, Johnson TN, Abduljalil K, Tucker GT, Rostami-Hodjegan A. A re-evaluation and validation of ontogeny functions for cytochrome P450 1A2 and 3A4 based on in vivo data. *Clin Pharmacokinet*. 2014;53:625-636.
31. Li G-F, Yu G, Li Y, Zheng Y, Zheng QS, Derendorf H. Quantitative estimation of plasma free drug fraction in patients with varying degrees of hepatic impairment: a methodological evaluation. *J Pharm Sci*. 2018;107:1948-1956.
32. Paine MF, Hart HL, Ludington SS, Haining RL, Rettie AE, Zeldin DC. The human intestinal cytochrome P450 "pie". *Drug Metab Dispos Biol Fate Chem*. 2006;34:880-886.
33. Yang J, Jamei M, Yeo KR, Tucker GT, Rostami-Hodjegan A. Prediction of intestinal first-pass drug metabolism. *Curr Drug Metab*. 2007;8:676-684.
34. Heimbach T, Chen Y, Chen J, et al. Physiologically-based pharmacokinetic modeling in renal and hepatic impairment populations: a pharmaceutical industry perspective. *Clin Pharmacol Ther*. 2021;110:297-310.
35. Gibbs MA, Hosea NA. Factors affecting the clinical development of cytochrome p450 3A substrates. *Clin Pharmacokinet*. 2003;42:969-984.
36. Jamei M, Marciniak S, Feng K, Barnett A, Tucker G, Rostami-Hodjegan A. The Simcyp population-based ADME simulator. *Expert Opin Drug Metab Toxicol*. 2009;5:211-223.
37. US FDA, C. for D. E. and bioequivalence studies with pharmacokinetic endpoints for drugs submitted under an abbreviated new drug application. US Food and Drug Administration. 2021.

https://www.fda.gov/regulatory-information/search-fda-guidance-documents/bioequivalence-studies-pharmacokinetic-endpoints-drugs-submitted-under-abbreviated-new-drug
38. Schmidt S, Gonzalez D, Derendorf H. Significance of protein binding in pharmacokinetics and pharmacodynamics. *J Pharm Sci*. 2010;99:1107-1122.
39. Regårdh CG. Factors contributing to variability in drug pharmacokinetics. IV. Renal excretion. *J Clin Hosp Pharm*. 1985;10:337-349.
40. Le J. Drug elimination – drugs. Merck Manual Consumer Version. 2022. https://www.merckmanuals.com/home/drugs/administration-and-kinetics-of-drugs/drug-elimination
41. Lin W, Chen Y, Unadkat JD, Zhang X, Wu D, Heimbach T. Applications, challenges, and outlook for PBPK modeling and simulation: a regulatory industrial and academic perspective. *Pharm Res*. 2022;39:1701-1731.
42. Han AN, Han BR, Zhang T, Heimbach T. Hepatic impairment physiologically based pharmacokinetic model development: current challenges. *Curr Pharmacol Rep*. 2021;7:213-226.
43. Stangier J, Stähle H, Rathgen K, Roth W, Shakeri-Nejad K. Pharmacokinetics and pharmacodynamics of dabigatran etexilate, an oral direct thrombin inhibitor, are not affected by moderate hepatic impairment. *J Clin Pharmacol*. 2008;48:1411-1419.

SUPPORTING INFORMATION

Additional supporting information can be found online in the Supporting Information section at the end of this article.

How to cite this article: Ladumor MK, Storelli F, Liang X, et al. Predicting changes in the pharmacokinetics of CYP3A-metabolized drugs in hepatic impairment and insights into factors driving these changes. *CPT Pharmacometrics Syst Pharmacol*. 2023;12:261-273. doi:10.1002/psp4.12901